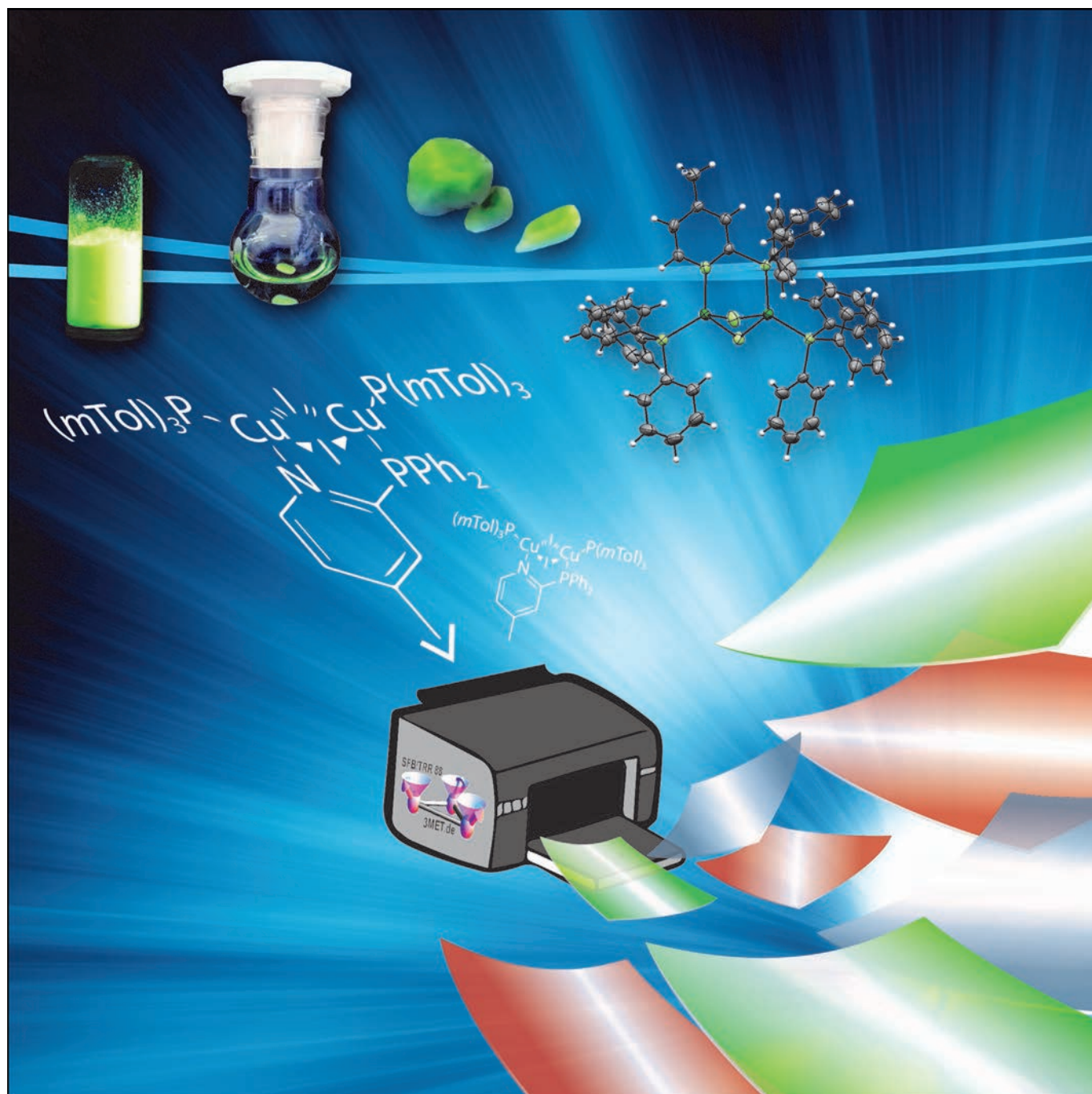


Towards Printed Organic Light-Emitting Devices: A Solution-Stable, Highly Soluble Cu^I-NHetPHOS** Complex for Inkjet Processing

Manuela Wallesch,^[a] Anand Verma,^[b] Charlotte Fléchon,^[b] Harald Flügge,^[b] Daniel M. Zink,^[b] Stefan M. Seifermann,^[b] José M. Navarro,^[b] Tonya Vitova,^[c] Jörg Göttlicher,^[d] Ralph Steininger,^[d] Lothar Weinhardt,^[d, e, f] Manuel Zimmer,^[g] Markus Gerhards,^[g] Clemens Heske,^{*,[d, e, f]} Stefan Bräse,^{*,[a]} Thomas Baumann,^[b] and Daniel Volz^{*,[b]}



Abstract: The development of iridium-free, yet efficient emitters with thermally activated delayed fluorescence (TADF) was an important step towards mass production of organic light-emitting diodes (OLEDs). Progress is currently impeded by the low solubility and low chemical stability of the materials. Herein, we present a Cu^I-based TADF emitter that is sufficiently chemically stable under ambient conditions and can be processed by printing techniques. The solubility is drastically enhanced (to 100 gL⁻¹) in relevant printing solvents. The integrity of the complex is preserved in solution, as was demonstrated by X-ray absorption spectroscopy and other techniques. In addition, it was found that the optoelectronic properties are not affected even when partly processing under ambient conditions. As a highlight, we present a TADF-based OLED device that reached an efficiency of 11 ± 2% external quantum efficiency (EQE).

Organic light-emitting diodes (OLEDs)^[1] are used in smartphones, tablet PCs, watches, and TVs. Room for improvement remains, in particular related to the availability and sustainability of their components.^[2] Phosphorescent, often iridium-based, materials are expensive and rare.^[3] Current processing tech-

niques based on vacuum deposition are elaborate and cannot be easily scaled up, which will likely slow down or even prevent the use of OLEDs in mass-produced applications, such as lighting and packaging. By using thermally activated delayed fluorescence (TADF), that is, singlet harvesting, instead of phosphorescence, progress has been demonstrated with devices exhibiting more than 20% external quantum efficiency (EQE).^[4,5] Metal-free materials,^[6-9] as well as Cu^I complexes,^[10,11] have been used for this purpose. However, problems associated with vacuum processing remain: Although there are first results with Cu^I complexes employing lab-scale processing techniques, such as spin coating, most organic TADF emitters are poorly soluble.^[12] To date, there are only limited results regarding the solution processing of metal-free TADF emitters, which is related to the high solubility required for industrial-scale printing. In some studies on 4CzIPN,^[8,13] solvents, such as dichloromethane and THF, were used,^[14,15] but those are too volatile for industrial printing. For well-soluble copper emitters, other problems arise. A recently introduced, promising Cu^I emitter with 16% EQE was shown to be vulnerable towards oxygen and water exposure.^[16] Also, the local structure found in crystalline phases is not necessarily the same as in solution or amorphous films: Due to the rich structural chemistry of Cu^I complexes, structurally stable complexes are required to suppress the formation of coexisting species.^[17] By using X-ray spectroscopy, it has also been demonstrated that for [Cu(N)₂]-type complexes processed under vacuum, species, such as [Cu(N)], may be formed.^[18] To resolve all of the above-discussed issues, a new NHetPHOS (N-heterocyclic phosphine)-type^[19] Cu^I complex was synthesized. The dinuclear Cu₂X₂ unit in these compounds leads to a rigid structure compared with mononuclear complexes, which in addition to a delocalization of the frontier orbitals causes improved photophysical properties due to cooperative effects.^[19]

Complex **1** was synthesized by using a slightly modified, simple procedure giving high yields (Figure 1; see the Supporting Information for details).^[20] The coordination compound mainly consists of commercially available CuI and ligands. Only a small fraction of the overall mass (22 wt%, MePyrPHOS ligand) had to be synthesized “in house”, thus, making the synthesis of the complex readily scalable. The largest batch in this study gave 40 g of **1** (90% yield). Similar to all dinuclear NHetPHOS complexes, **1** contains a butterfly-shaped Cu₂I₂ unit, a bridging N,P ligand with a nitrogen-containing heterocycle (NHet), and two additional monodentate P donors with tris-*m*-tolylphosphine (P(*m*Tol)₃; Figure 1).

The *ortho* isomer of this ligand cannot be incorporated into the NHetPHOS structure, whereas the *para* isomer has already been synthesized and published by our group.^[20,21] It is striking that the solubility of **1** is much higher than for the *para* counterpart. We also note that numerous attempts to grow single crystals for X-ray diffraction were not successful, but we were

[a] Dr. M. Wallesch, Prof. Dr. S. Bräse

Institute of Toxicology and Genetics and
Institute of Organic Chemistry, Karlsruhe Institute of Technology
Kaiserstrasse 12, 76131 Karlsruhe (Germany)
E mail: braese@kit.edu

[b] A. Verma, Dr. C. Fléchon, Dr. H. Flügge, Dr. D. M. Zink, Dr. S. M. Seifermann,

Dr. J. M. Navarro, Dr. T. Baumann, Dr. D. Volz
CYNORA GmbH, Werner von Siemensstrasse 2 6, 76646 Bruchsal (Germany)
E mail: volz@cynora.com

[c] Dr. T. Vitova

Institute for Nuclear Waste Disposal (INE)
Karlsruhe Institute of Technology, P.O. 3640, 76021 Karlsruhe (Germany)

[d] Dr. J. Göttlicher, Dr. R. Steininger, Dr. L. Weinhardt, Prof. Dr. C. Heske

Institute for Photon Science and Synchrotron Radiation
Karlsruhe Institute of Technology
Hermann von Helmholtz Platz 1
76344 Eggenstein Leopoldshafen (Germany)
E mail: heske@kit.edu

[e] Dr. L. Weinhardt, Prof. Dr. C. Heske

Institute for Chemical Technology and Polymer Chemistry (ITCP)
Karlsruhe Institute of Technology
Engesserstrasse 18/20, 76128 Karlsruhe (Germany)

[f] Dr. L. Weinhardt, Prof. Dr. C. Heske

Department of Chemistry and Biochemistry, University of Nevada
Las Vegas (UNLV), 4505 Maryland Pkwy, Las Vegas, NV 89154 4003 (USA)
E mail: heske@unlv.nevada.edu

[g] M. Zimmer, Prof. Dr. M. Gerhards

University of Kaiserslautern
Chemistry Department and Research Center OPTIMAS
Erwin Schrödinger Strasse 52, 67663 Kaiserslautern (Germany)

[**] NHetPHOS = N heterocyclic phosphine.

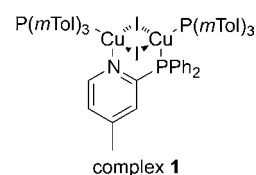


Figure 1. Molecular structure of complex **1**.

able to crystallize the *para* derivative and determine its structure.^[20] Table S2–1 in the Supporting Information contains solubility data for **1** in various solvents, both with low (e.g., toluene) and high (e.g., indane) boiling points. For instance, the solubility of **1** in toluene and chlorobenzene is >30 and >100 mg mL⁻¹, respectively, whereas the solubility of the *para* derivative was significantly lower (1 and 20 mg mL⁻¹).^[20,21] We assign this behavior to the lower symmetry of the *meta*-tolyl-substituents, which is being discussed in the Supporting Information in detail. The extraordinarily high solubility of **1** facilitates the development of inks for printing processes.

Photophysical properties of complex **1** were investigated in various sample forms (Figure 2). All data and an in-depth discussion, also concerning the TADF properties of the compound, are given in the Supporting Information. The TADF nature of NHetPHOS was recently established in an in-depth study by temperature-dependent spectroscopy.^[22,23] In general, the emission spectra are relatively broad and unstructured, which indicates a charge-transfer nature of the emitting state. This was supported by detailed quantum-chemical studies, showing that NHetPHOS emitters typically exhibit a (M+XLCT)-type emission.^[20,24,25] The emission maximum of complex **1** was found to be at 550 nm, independent of the solid-state environment (i.e., amorphous powder vs. neat film vs. poly(methyl methacrylate) (PMMA) matrix, top panel in Figure 2). The compound showed a high photoluminescence quantum yield (Φ_{PL}) of $75 \pm 5\%$ in the solid state as neat powder, which drops to $57 \pm 5\%$ and $56 \pm 5\%$ for the neat film and the PMMA matrix, respectively. In PYD2, the yields are slightly higher (62 and $60 \pm 5\%$ for the 40% and 20% concentration, respectively). The calculated radiative and non-radiative kinetic rates k_r and k_{nr} which are given in the Supporting Information, indicate little differences among the different film samples, but more significant changes between powder and film, as has been also recently found for other NHetPHOS compounds.^[21]

As was expected,^[21,24] the photophysical behavior of complex **1** in solution deviates from the behavior in solid samples. The absorption spectra are broad and unstructured (Figure 2, center). The comparison between absorption and excitation spectra (Figure 2, bottom left), which were recorded for the peak emission of the PL spectra (Figure 2, bottom right) suggests that the (M+XLCT) transition is associated with a weak absorption shoulder in the region between 300 and 310 nm. This is indicative for a low oscillator strength, and therefore, a low probability of the vertical transition between the S_0 and S_1 state. Both the extinction and the position of the band seem to be a function of the solvents' permittivity ϵ , which was analyzed in the Supporting Information in details. The Φ_{PL} of complex **1** in aerated solution was very low in each solvent ($<2\%$), which did not give a reliable determination of the emission decay time. These drastic changes might be caused by dissociation equilibria and the formation of different coexisting species, which could be linked to the dielectric constant of the environment, or the effects of the matrix on the electronic structure of the molecules. To clarify whether the former can be excluded, the molecular structure was investigated by

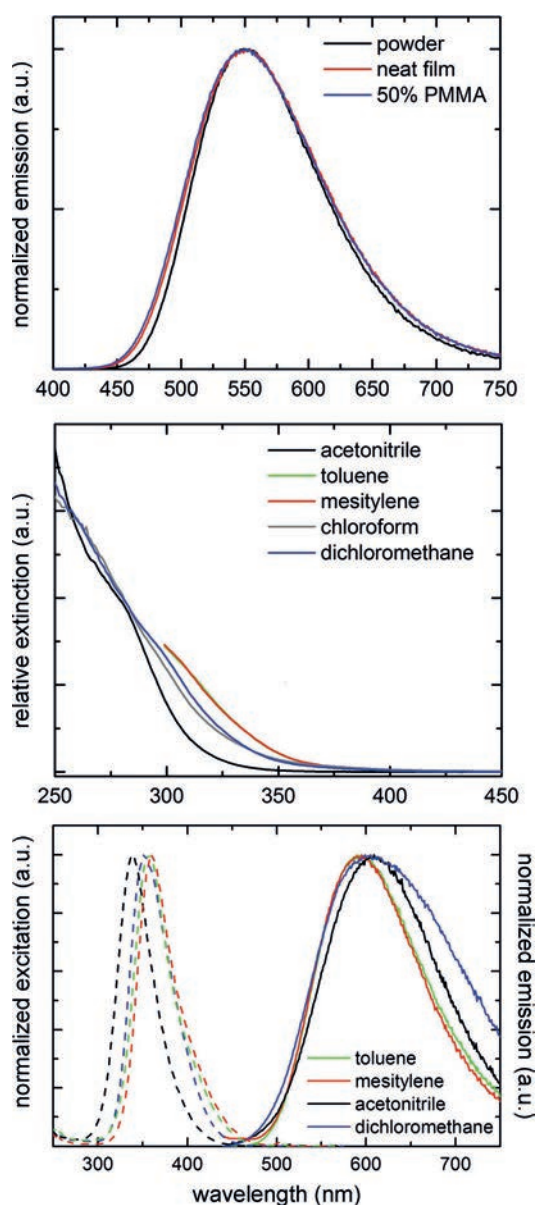


Figure 2. Top: Photoluminescence (PL) spectra of complex **1** in different solid environments (top panel: powder, neat film, and a 1:1 mixture of PMMA and the emitting compound). Middle: Normalized absorption spectra of complex **1** in different solvents (1 mg mL⁻¹ solution). Spectra for toluene and mesitylene are not shown for $\lambda < 300$ nm due to self absorption of these solvents. Bottom: Excitation (dashed) and PL (solid lines) spectra of complex **1** in different solvents. Emission spectra overlap for toluene and mesitylene.

NMR, Fourier-transformation infrared (FT-IR) technique, and synchrotron-based X-ray absorption spectroscopy (XAS).

NMR spectra of complex **1** in various solvents were recorded (see the Supporting Information). As known for NHetPHOS complexes^[20,26] and other copper(I) complexes,^[17,27,28] ¹H NMR spectra are slightly broadened due to a certain degree of flexibility of the structure in solution.

Unlike reported for other heteroleptic compounds,^[17] we noticed no additional signal sets. Due to the large number of nonequivalent C atoms per complex molecule, no satisfying ¹³C NMR spectra could be recorded. Even with the ¹H NMR

spectra being indicative for the presence of only one species regardless of the solvent, the determination of the structure of these species was not possible due to the broadness of the spectra. Because of this, further spectroscopic analyses were performed: full IR spectra (in solid state and different solvents, including the C–H stretch region) can be found in the Supporting Information. In brief, all features, most prominently the C=C stretch vibrations at approximately 1600 cm^{-1} , the scissoring and rocking vibrations at approximately 1500 cm^{-1} , the aromatic C–H scissoring vibrations at approximately 1100 cm^{-1} , and the aromatic C–H wagging vibrations at approximately 800 cm^{-1} , found in a powder sample of complex **1**, were also present in the CCl_4 solution spectra (except aromatic C–H wagging due to self-absorption of CCl_4). No additional bands were identified, which further supports the conclusions drawn from the ^1H NMR data.

To probe the local coordination geometry of the Cu^{I} centers in **1**, XAS at the Cu_k edge was employed. The extended X-ray absorption fine structure (EXAFS) region gave insights on the number and type of nearest-neighbor atoms, the coordination geometry, and bond lengths (Figure 3 and the Supporting Information). Information on the oxidation state, as well as on the coordination environment and symmetry of the copper ion, can be extracted from the X-ray absorption near-edge structure (XANES) region (the full analysis is discussed in the Supporting Information). In short, the interatomic distances and coordination numbers are very similar within the uncertainties for all studied samples. Minor changes in MeCN were found, which is discussed in the Supporting Information. From the XANES and EXAFS analyses of the powder and solution samples of complex **1**, we conclude that the coordination geometry around the copper(I) centers, as well as the type of the nearest-neighbor atoms and the interatomic distances, are very similar for all samples.

After comparison of solid amorphous powder, thin film, and solution samples with X-ray absorption, as well as NMR and FTIR data, we verified within the accuracy of these methods that the structure of complex **1** is retained during the entire inkjet processing chain as long as noncoordinating solvents are employed. Our results suggest that complex **1** is significantly more stable upon processing than cationic, mononuclear compounds, which dissociate to a degree evident by NMR spectroscopy.^[17] In fact, the structure of complex **1** is retained in noncoordinating solvents within the accuracy of the methods described above.

To date, we have demonstrated that complex **1** has a very high solubility in various solvents, attractive photophysical properties in neat and doped thin films, and is reasonably stable. On due course is an evaluation of spin-coated and inkjet-printed OLED devices. Three sets of experiments were conducted. First, we compared the impact of ambient air and oxygen on the properties of OLEDs with non-doped emission layers of complex **1**, which were made by spin coating from chlorobenzene and *o*-xylene (**A-1** to **A-4**). Then, we used the same stack architecture to process devices with inkjet printing from indane, as well as an indane-mesitylene mixture (**B-1** and **B-2**).

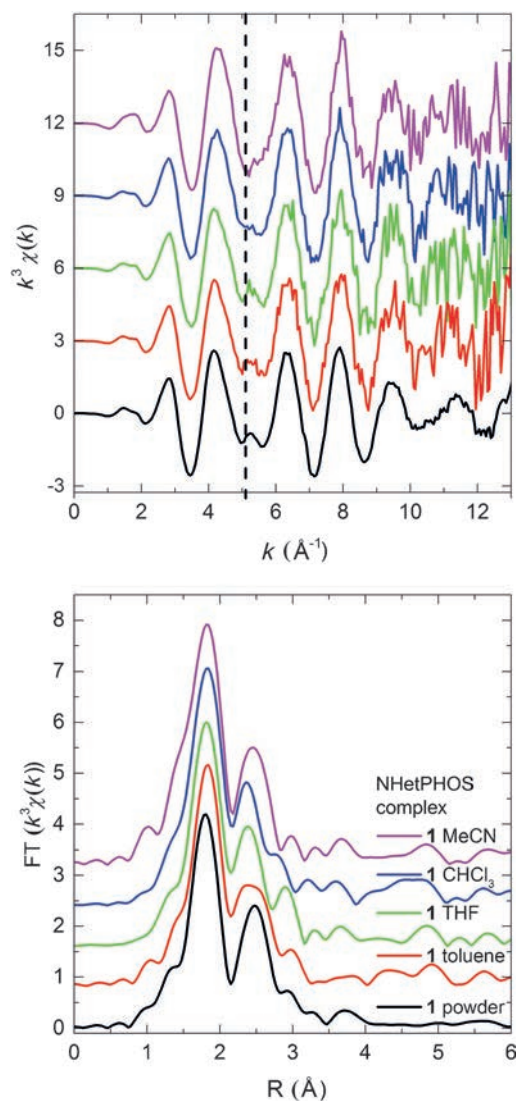


Figure 3. Top: $k^3\chi(k)$ and bottom: $FT[k^3\chi(k)]$ EXAFS data of powder and solution samples of complex **1**. The marker at 5.1 \AA^{-1} in the top panel indicates differences between the samples (the color code is given in the bottom panel).

Lastly, we evaluated the potential of complex **1** by adding PYD2, a high-triplet-energy host material in a doped emission layer (device **C**). The results are summarized in the Supporting Information and Table 1. We chose a simple-stack architecture without a hole transport layer, which would have required optimization of an additional printing step and, potentially, even the application of crosslinking techniques (Figure 4). We processed the emission layer directly on PEDOT:PSS (poly(3,4-ethylenedioxythiophene) polystyrene sulfonate), and used the solvents *ortho*-xylene (b.p. $144\text{ }^\circ\text{C}$), chlorobenzene (b.p. $131\text{ }^\circ\text{C}$), mesitylene (b.p. $164\text{ }^\circ\text{C}$), and indane (b.p. $177\text{ }^\circ\text{C}$) at concentrations between 8 and 12 mg mL^{-1} .

The results presented in Table 1 and Figure 5 indicate that the optoelectronic performance of the devices was not affected by the presence of ambient air during the processing of the emission layer with **A-1** to **A-4**: the measured performance was within the expected range in all cases. Using inkjet print-

Table 1. Device results.

No.	Processing	Solvent	Conditions ^[b]	$V_{\text{turn on}}$ [V]	EQE_{max}	$\eta_{\text{c,max}}$ [cd A ⁻¹]	$\eta_{\text{p,max}}$ [lm W ⁻¹]	B_{max} [cd m ⁻²]	λ_{max} [nm]
A 1	SC ^[a] , neat EML	chlorobenzene	g/g	3.7 ± 0.2	8.0 ± 0.1	24.4 ± 0.3	15.3 ± 0.2	42 000	553
A 2	SC, neat EML	chlorobenzene	a/a	3.5 ± 0.2	7.8 ± 0.5	24.9 ± 1.8	15.9 ± 1.4	40 000	553
A 3	SC, neat EML	<i>o</i> xylene	g/g	3.8 ± 0.2	7.8 ± 0.1	24.5 ± 0.5	15.6 ± 0.3	40 000	553
A 4	SC, neat EML	<i>o</i> xylene	a/a	3.4 ± 0.2	7.9 ± 0.2	24.6 ± 0.8	16.6 ± 0.5	35 000	552
B 1	IJP ^[b] , neat EML	indane	a/a	4.0 ± 0.2	2.1 ± 0.8	7.3 ± 2.5	4.5 ± 2.1	1600	550
B 2	IJP, neat EML	indane/mesitylene	a/a	3.7 ± 0.2	4.7 ± 0.6	15.2 ± 1.4	8.7 ± 1.3	3000	550
C	SC, doped EML	toluene	g/g	3.7 ± 0.2	11.4 ± 1.9	36.4 ± 6.4	21.8 ± 8.2	34 000	552

[a] SC = spin coated; IJP = inkjet printed. [b] First letter indicates conditions for processing, second for drying; g = glovebox; a = air.

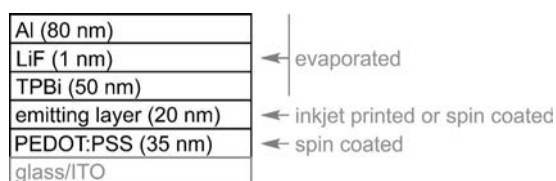


Figure 4. OLED architecture used for printing studies.

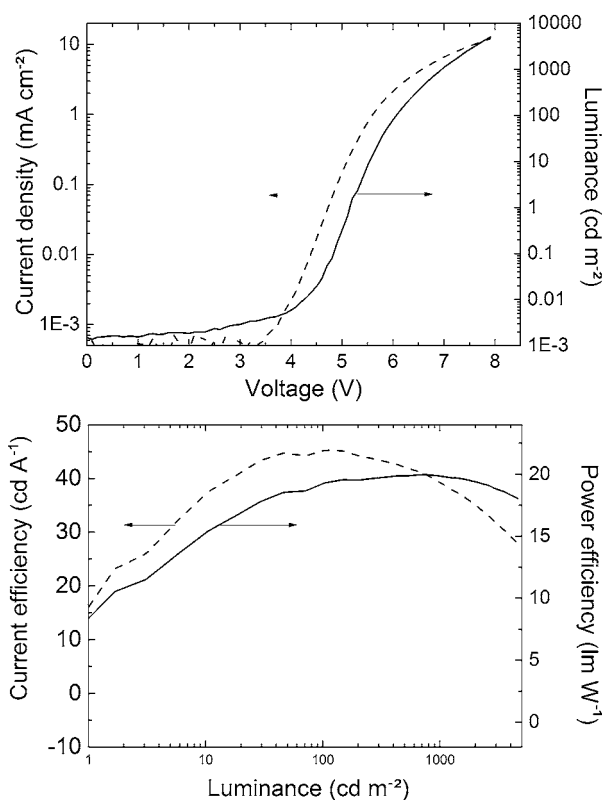


Figure 5. L/I/V and efficiency/luminance curves for device C. Electroluminescence spectra and further data are given in the Supporting Information.

ing instead of spin coating leads to a slight reduction of the performance in **B-1** and **B-2**. As was pointed out in the section above, inks prepared from complex **1** were stable for several hours in air-saturated solution. Thus, we attribute these changes to solvent effects and effects caused by the morphology of the emitting layer, which can be further optimized empirically.

OLED **C** outlines strategies to further improve the performance up to 11.4 ± 1.9% EQE in a doped, spin-coated device. At 8 V driving voltage, a record brightness of 34 000 cd m⁻² was reached. Due to reduced concentration quenching, the efficiency roll-off of device **C** is much less pronounced than for comparable NHetPHOS compounds,^[29] especially considering the early development stage of this stack architecture. The key for this is an optimization of all layer thickness, as well as the introduction of a host material.

We note that the operational stability of the devices with complex **1** was not investigated in this study. Although all devices were stable enough to be properly analyzed, more work needs to be done to reach a satisfactory stability level. Specifically, complex **1** seems to transport holes much better than electrons. It is thus necessary to find a device architecture that reduces the hole current, which is transported by the emitter, because this is likely to be problematic. An indication for this is the occurrence of irreversible oxidation in cyclic voltammetry experiments,^[30] which suggests that hole transport in an OLED is also irreversible. Apart from the optimization of the drying conditions, it is thus prudent to develop an optimized device architecture that enables both efficient and stable devices.

In summary, a new highly efficient NHetPHOS Cu^I emitter was synthesized. Complex **1** was characterized chemically and photophysically. The new TADF-material is soluble in a broad range of different solvents relevant for inkjet printing. By using IR, NMR spectroscopy, as well as synchrotron-based X-ray absorption spectroscopy, we proved that the profound changes of the photophysics in solution compared with solid-state results are—unlike what was established for other Cu^I complexes—not a result of dissociation or degradation. In an extensive OLED study, we showed that the material is not only stable in ink formulations, but can also be processed in the presence of ambient air with spin coating, as well as inkjet-printing, even in the absence of a host material. In a refined device, efficiency values of more than 11% EQE and ultrahigh brightness values of 34 000 cd m⁻² were obtained.

Acknowledgements

Financial support from the Deutsche Forschungsgemeinschaft (DFG) by support for the transregional collaborative research center SFB/TRR 88 „3MET“ projects B2 and C2, the BioInterfaces

and MML programs of the Helmholtz-Association, and the Deutsche Telekom Stiftung are acknowledged. This work has been sponsored by the German Federal Ministry of Education and Research (BMBF) in the funding programs „cyCESH“ and „cyFLEX“.

Keywords: copper · organic light-emitting diodes (OLEDs) · thermally activated delayed fluorescence (TADF) · X-ray absorption spectroscopy

- [1] C. W. Tang, S. A. VanSlyke, *Appl. Phys. Lett.* **1987**, *51*, 913.
- [2] D. Volz, M. Wallesch, C. Fléchon, M. Danz, A. Verma, J. M. Navarro, D. M. Zink, S. Bräse, T. Baumann, *Green Chem.* **2015**, *17*, 1988–2011.
- [3] N. N. Greenwood, A. Earnshaw, *Chemistry of the Elements*, Butterworth, **1997**.
- [4] V. Jankus, P. Data, D. Graves, C. McGuinness, J. Santos, M. R. Bryce, F. B. Dias, A. P. Monkman, *Adv. Funct. Mater.* **2014**, *24*, 6178–6186.
- [5] Q. Zhang, D. Tsang, H. Kuwabara, Y. Hatae, B. Li, T. Takahashi, S. Y. Lee, T. Yasuda, C. Adachi, *Adv. Mater.* **2015**, *27*, 2096–2100.
- [6] Q. Zhang, B. Li, S. Huang, H. Nomura, H. Tanaka, C. Adachi, *Nat. Photonics* **2014**, *8*, 326–332.
- [7] K. Goushi, K. Yoshida, K. Sato, C. Adachi, *Nat. Photonics* **2012**, *6*, 253–258.
- [8] H. Uoyama, K. Goushi, K. Shizu, H. Nomura, C. Adachi, *Nature* **2012**, *492*, 234–238.
- [9] A. Kretzschmar, C. Patze, S. T. Schwaebel, U. H. F. Bunz, *J. Org. Chem.* **2015**, *80*, 9126–9131.
- [10] H. Yersin, A. F. Rausch, R. Czerwieńiec, T. Hofbeck, T. Fischer, *Coord. Chem. Rev.* **2011**, *255*, 2622–2652.
- [11] R. Czerwieńiec, J. Yu, H. Yersin, *Inorg. Chem.* **2011**, *50*, 8293–8301.
- [12] Y. J. Cho, K. S. Yook, J. Y. Lee, *Adv. Mater.* **2014**, *26*, 6642–6646.
- [13] M. P. Gaj, C. Fuentes Hernandez, Y. Zhang, S. R. Marder, B. Kippelen, *Org. Electron.* **2015**, *16*, 109–112.
- [14] R. Komatsu, H. Sasabe, S. Inomata, Y. J. Pu, J. Kido, *Synth. Met.* **2015**, *202*, 165–168.
- [15] Y. Suzuki, Q. Zhang, C. Adachi, *J. Mater. Chem. C* **2015**, *3*, 1700–1706.
- [16] J. C. Deaton, S. C. Switalski, D. Y. Kondakov, R. H. Young, T. D. Pawlik, D. J. Giesen, S. B. Harkins, A. J. M. Miller, S. F. Mickenberg, J. C. Peters, *J. Am. Chem. Soc.* **2010**, *132*, 9499–9508.
- [17] A. Kaeser, M. Mohankumar, J. Mohanraj, F. Monti, M. Holler, J. J. Cid, O. Moudam, I. Nierengarten, L. Karmazin Brelot, C. Duhayon, *Inorg. Chem.* **2013**, *52*, 12140–12151.
- [18] Z. Liu, M. F. Qayyum, C. Wu, M. T. Whited, P. I. Djurovich, K. O. Hodgson, B. Hedman, E. I. Solomon, M. E. Thompson, *J. Am. Chem. Soc.* **2011**, *133*, 3700–3703.
- [19] M. Wallesch, D. Volz, D. M. Zink, U. Schepers, M. Nieger, T. Baumann, S. Bräse, *Chem. Eur. J.* **2014**, *20*, 6578–6590.
- [20] D. Volz, D. M. Zink, T. Bocksrocker, J. Friedrichs, M. Nieger, T. Baumann, U. Lemmer, S. Bräse, *Chem. Mater.* **2013**, *25*, 3414–3426.
- [21] D. Volz, M. Wallesch, S. L. Grage, J. Göttlicher, R. Steininger, D. Batchelor, T. Vitova, A. S. Ulrich, C. Heske, L. Weinhardt, *Inorg. Chem.* **2014**, *53*, 7837–7847.
- [22] M. J. Leitl, D. M. Zink, A. Schinabeck, T. Baumann, D. Volz, H. Yersin, *Top. Curr. Chem.* **2016**, *374*, 25.
- [23] L. Bergmann, D. M. Zink, S. Bräse, T. Baumann, D. Volz, *Top. Curr. Chem.* **2016**, *374*, 22.
- [24] D. M. Zink, M. Bächle, T. Baumann, M. Nieger, M. Kühn, C. Wang, W. Kloppe, U. Monkowius, T. Hofbeck, H. Yersin, *Inorg. Chem.* **2013**, *52*, 2292–2305.
- [25] D. M. Zink, D. Volz, T. Baumann, M. Mydlak, H. Flügge, J. Friedrichs, M. Nieger, S. Bräse, *Chem. Mater.* **2013**, *25*, 4471–4486.
- [26] D. Volz, T. Baumann, H. Flügge, M. Mydlak, T. Grab, M. Bächle, C. Barner-Kowollik, S. Bräse, *J. Mater. Chem.* **2012**, *22*, 20786.
- [27] O. Crespo, M. C. Gimeno, A. Laguna, C. Larraz, *Z. Naturforsch. Sect. B* **2009**, *64*, 1525–1534.
- [28] O. Moudam, A. Kaeser, B. Delavaux Nicot, C. Duhayon, M. Holler, G. Accorsi, N. Armaroli, I. Ségué, J. Navarro, P. Destruel, *Chem. Commun.* **2007**, *29*, 3077–3079.
- [29] D. Volz, Y. Chen, M. Wallesch, R. Liu, C. Fléchon, D. M. Zink, J. Friedrichs, H. Flügge, R. Steininger, J. Göttlicher, *Adv. Mater.* **2015**, *27*, 2538–2543.
- [30] A. M. Leiva, L. Rivera, B. Loeb, *Polyhedron* **1991**, *1*, 347–350.

Repository KITopen

Dies ist ein Postprint/begutachtetes Manuskript.

Empfohlene Zitierung:

Wallesch, M.; Verma, A.; Fléchon, C.; Flügge, H.; Zink, D. M.; Seifermann, S. M.; Navarro, J. M.; Vitova, T.; Göttlicher, J.; Steininger, R.; Weinhardt, L.; Zimmer, M.; Gerhards, M.; Heske, C.; Bräse, S.; Baumann, T.; Volz, D.

[Towards Printed Organic Light-Emitting Devices: A Solution-Stable, Highly Soluble Cu-NHetPHOS](#)

2016. Chemistry - a European journal, 22 (46), 16400–16405.

[doi:10.5445/IR/1000061608](https://doi.org/10.5445/IR/1000061608)

Zitierung der Originalveröffentlichung:

Wallesch, M.; Verma, A.; Fléchon, C.; Flügge, H.; Zink, D. M.; Seifermann, S. M.; Navarro, J. M.; Vitova, T.; Göttlicher, J.; Steininger, R.; Weinhardt, L.; Zimmer, M.; Gerhards, M.; Heske, C.; Bräse, S.; Baumann, T.; Volz, D.

[Towards Printed Organic Light-Emitting Devices: A Solution-Stable, Highly Soluble Cu-NHetPHOS](#)

2016. Chemistry - a European journal, 22 (46), 16400–16405.

[doi:10.1002/chem.201603847](https://doi.org/10.1002/chem.201603847)